SCATTERING OF A HERMITE-GAUSSIAN BEAM BY A CHIRAL SPHERE

Mitsuhiro YOKOTA
Department of Electrical and Electronic Engineering
Miyazaki University, Miyazaki, 889-2192, Japan
E-mail: yokota@esl.miyazaki-u.ac.jp

Sailing HE
Department of Electromagnetic Theory
Royal Institute of Technology, S-100 44 Stockholm, Sweden
E-mail: sailing@tet.kth.se

Takashi TAKENAKA
Department of Electrical and Electronic Engineering
Nagasaki University, Nagasaki, 852-8521, Japan
E-mail: takenaka@net.nagasaki-u.ac.jp

1. Introduction

Chiral medium has attracted attention due to many associated interesting phenomena in optical and electromagnetic activity and its potential applications in various fields [1]. Recently, the phenomena of wave interaction with chiral structures such as chiral sphere [2], stratified chiral slab [3], and chiral grating [4] [5] have been examined theoretically.

The electromagnetic field radiated from waveguide horns and laser cavities is an approximately beam-like field. Thus, propagation and scattering problems of a beam field are of practical importance. One of the methods for treating the beam field is the complex-source-point method [6] [7].

In this paper, we investigate the scattering of the Hermite-Gaussian beam by a chiral sphere. The Hermite-Gaussian beam can be expressed as the superpositions of multipole fields at complex source points [8] in the paraxial region. The electromagnetic fields are expanded in terms of the vector spherical wave functions [9] [10], and the unknown coefficients for the internal field and the scattered field are determined by the boundary conditions on the surface of the chiral sphere. As numerical examples, the near fields for the lowest-order incident beam are calculated and compared with those for a plane wave incidence.

2. Hermite-Gaussian beam generated by multipole fields at a complex source point

For the scattering of a beam field, the complex-source-point method is one of the useful methods. The time factor $\exp(-i\omega t)$ is suppressed throughout. The electromagnetic fields radiated from the source point located at the complex point $(-x_0, -y_0, -z_0 + ib)$ are represented as

$$\mathbf{E} = \frac{i}{\omega\mu\varepsilon}\nabla \times \nabla \times \mathbf{A} \tag{1}$$

$$\mathbf{H} = \frac{1}{\mu}\nabla \times \mathbf{A} \tag{2}$$

The vector potential $\mathbf{A}$ is given by

$$\mathbf{A} = \widehat{x}\,\frac{e^{ik_0R}}{ik_0R} \tag{3}$$

where $R(= \sqrt{(x+x_0)^2 + (y+y_0)^2 + (z+z_0-ib)^2})$ is the distance between the observation point (x, y, z) and the source point, $\widehat{x}$ is the unit vector in the polarization direction and $k_0(= 2\pi/\lambda)$ is the wavenumber in free space. The branch of R is chosen such that $R \to z$ as $z \to \infty$ in order to satisfy the radiation conditions. b is related with the smallest spot size $w_0(= \sqrt{2b/k})$ of the lowest-order beam field. When the observation point is far away from the branch point and in the paraxial region, the electromagnetic fields become Gaussian beams [10].

The Hermite-Gaussian beam field can be generated by the multipole fields located at the complex source point as follows [7]:

$$\mathbf{A}_{\mu,\nu} = \widehat{x}\,\frac{\partial^{\mu+\nu}}{\partial x^{\mu}\partial y^{\nu}}\,\frac{e^{ikR}}{ikR} \tag{4}$$

The multipole fields are related with the complex beam proposed by Siegman [11], and the complex beam is related with the conventional one [8]. By using these relations, the conventional Hermite-Gaussian beam field $\psi_{\mu,\nu}$ is expressed as a superposition of a finite number of multipole fields under the paraxial approximation [8]:

$$\widehat{x}\,\psi_{\mu,\nu} \sim kb\,e^{-kb}\sqrt{\frac{2\mu!\nu!}{\pi}}\,e^{ik(z+z_0)}\sum_{p=0}^{[\mu/2]}\sum_{q=0}^{[\nu/2]}\frac{2^{-p+q}(-w_0)^{\mu+\nu-2(p+q)}}{w_0\,p!q!(\mu-2p)!(\nu-2q)!}\,\mathbf{A}_{\mu-2p,\nu-2q} \tag{5}$$

Therefore, we investigate the scattered field for a multipole field $\mathbf{A}_{\mu,\nu}$ in the next section.

3. Scattering by a chiral sphere

Let a multipole field $\mathbf{A}_{\mu,\nu}$ be incident upon a chiral sphere shown in Fig. 1. The incident beam has the smallest spot size w_0 at the beam waist $(-x_0, -y_0, -z_0)$. The chiral sphere (with radius a) has relative permitivity ε_r, relative permiability μ_r, nonreciprocity parameter χ and chirality parameter κ.

The constitutive relations for a nonreciprocal chiral medium are given by [1]

$$\mathbf{D} = \varepsilon_0\varepsilon_r\mathbf{E} + \xi\mathbf{H} \tag{6}$$

$$\mathbf{B} = \zeta\mathbf{E} + \mu_0\mu_r\mathbf{H} \tag{7}$$

where

$$\xi = (\chi + i\kappa)\sqrt{\varepsilon_0\mu_0} \tag{8}$$

$$\zeta = (\chi - i\kappa)\sqrt{\varepsilon_0\mu_0} \tag{9}$$

ε_0 and μ_0 are permitivity and permiability in the free space, respectively. The nonreciprocity parameter and chirality parameter are governed by the following inequality,

$$\chi^2 + \kappa^2 < \varepsilon_r\mu_r \tag{10}$$

The multipole field $\mathbf{A}_{\mu,\nu}$ can be expanded in terms of the vector spherical wave functions. By using this expansion and Eqs. (1) and (2), the incident electromagnetic fields are obtained as follows [10]:

$$\mathbf{E}^{inc} = i\omega\sum_{l=1}^{+\infty}\sum_{-l}^{l}\left[\alpha^{(\eta)}(\mu,\nu:l,m)\,\mathbf{M}^{(s)}_{l,m}(k_0,\mathbf{r}) + \beta^{(\eta)}(\mu,\nu:l,m)\,\mathbf{N}^{(s)}_{l,m}(k_0,\mathbf{r})\right] \tag{11}$$

$$\mathbf{H}^{inc} = \frac{ik}{\mu}\sum_{l=1}^{+\infty}\sum_{-l}^{l}\left[\alpha^{(\eta)}(\mu,\nu:l,m)\,\mathbf{N}^{(s)}_{l,m}(k_0,\mathbf{r}) - \beta^{(\eta)}(\mu,\nu:l,m)\,\mathbf{M}^{(s)}_{l,m}(k_0,\mathbf{r})\right], \quad \eta \text{ and } s = 1,2 \tag{12}$$

where

$$\mathbf{M}^{(s)}_{l,m}(k,\mathbf{r}) = \nabla\times\left[\mathbf{r}Z^{(s)}_l(kr)Y^m_l(\theta,\phi)\right] \tag{13}$$

$$\mathbf{N}^{(s)}_{l,m}(k,\mathbf{r}) = \frac{1}{ik}\nabla\times\mathbf{M}^{(s)}_{l,m}(k,\mathbf{r}) \tag{14}$$

and the superscripts η and s are determined by the addition theorem. The functions $Z^{(1)}_l(kr)$ and $Z^{(2)}_l(kr)$ denote, respectively, the spherical Bessel function $j_l(kr)$ and the first-kind spherical Hankel function $h^{(1)}_l(kr)$. The function $Y^m_l(\theta,\phi)$ is defined by [9]

$$Y^m_l(\theta,\phi) = \sqrt{\frac{2l+1}{4\pi}\,\frac{(l-|m|)!}{(l+|m|)!}}P^{|m|}_l(\cos\theta)\,e^{im\phi} \tag{15}$$

and $P^{|m|}_l$ is the associated Legendre function of degree l and index m. The coefficients $\alpha^{(\eta)}(\mu,\nu:l,m)$ and $\beta^{(\eta)}(\mu,\nu:l,m)$ can be obtained by using the recurrence relations [10].

For a chiral sphere, there exist two eigenvalues k^+ and k^- given by

$$k^{\pm} = \omega\sqrt{\varepsilon_0\mu_0}\left(\sqrt{\varepsilon_r\mu_r - \chi^2} \pm \kappa\right) \tag{16}$$

The electric field in the sphere can be expanded in terms of the vector spherical wave functions with the arguments $k^{\pm}$ as

$$\mathbf{E}^{chi} = \sum_{l=1}^{+\infty} \sum_{m=-l}^{l} \left[a_{l,m}\, \mathbf{P}_{l,m}^{(1)}(k^{+}, \mathbf{r}) + b_{l,m}\, \mathbf{Q}_{l,m}^{(1)}(k^{-}, \mathbf{r}) \right] \tag{17}$$

where

$$\mathbf{P}_{l,m}^{(s)}(k, \mathbf{r}) = \mathbf{M}_{l,m}^{(s)}(k, \mathbf{r}) + i\, \mathbf{N}_{l,m}^{(s)}(k, \mathbf{r}) \tag{18}$$

$$\mathbf{Q}_{l,m}^{(s)}(k, \mathbf{r}) = \mathbf{M}_{l,m}^{(s)}(k, \mathbf{r}) - i\, \mathbf{N}_{l,m}^{(s)}(k, \mathbf{r}), \qquad s = 1, 2 \tag{19}$$

The scattered field of the multipole field $\mathbf{A}_{\mu,\nu}$ are expressed in terms of $\mathbf{P}_{l,m}^{(2)}(k_0, \mathbf{r})$ and $\mathbf{Q}_{l,m}^{(2)}(k_0, \mathbf{r})$,

$$\mathbf{E}^{sct} = \sum_{l=1}^{+\infty} \sum_{m=-l}^{l} \left[c_{l,m} \mathbf{P}_{l,m}^{(2)}(k_0, \mathbf{r}) + d_{l,m} \mathbf{Q}_{l,m}^{(2)}(k_0, \mathbf{r}) \right] \tag{20}$$

The boundary condition is for the tangential electromagnetic fields. The tangential electromagnetic fields of the incident beam can be obtained as follows,

$$\widehat{x} \times \mathbf{E}^{inc} = \sum_{l=1}^{+\infty} \sum_{m=-l}^{l} \left[\alpha_{l,m}^{inc}\, \mathbf{G}_{l,m}(\theta, \phi) + \beta_{l,m}^{inc}\, \mathbf{R}_{l,m}(\theta, \phi) \right] \tag{21}$$

$$\widehat{x} \times \mathbf{H}^{inc} = \sum_{l=1}^{+\infty} \sum_{m=-l}^{l} \left[\gamma_{l,m}^{inc}\, \mathbf{G}_{l,m}(\theta, \phi) + \delta_{l,m}^{inc}\, \mathbf{R}_{l,m}(\theta, \phi) \right] \tag{22}$$

where

$$\mathbf{G}_{l,m}(\theta, \phi) = \frac{1}{\sqrt{l(l+1)}} \nabla_{S_1} Y_l^m \tag{23}$$

$$\mathbf{R}_{l,m}(\theta, \phi) = \widehat{x} \times \mathbf{G}_{l,m} \tag{24}$$

The functions $\mathbf{G}_{l,m}(\theta, \phi)$ and $\mathbf{R}_{l,m}(\theta, \phi)$ are the tangential basis functions and form an orthonormal basis on the unit sphere S_1 [9]. The coefficients $\alpha_{l,m}^{inc}, \beta_{l,m}^{inc}, \gamma_{l,m}^{inc},$ and $\delta_{l,m}^{inc}$ are expressed in terms of $\alpha^{(\eta)}(\mu, \nu : l, m)$ and $\beta^{(\eta)}(\mu, \nu : l, m)$ by using Eqs. (11) and (12). The tangential electromagnetic fields inside and outside the sphere can be obtained in the same way. From the continuity of the tangential electromagnetic field, we obtain the unknown coefficients $a_{l,m}, b_{l,m}, c_{l,m},$ and $d_{l,m}$.

4. Numerical results

In this paper, the incident beam is assumed to be the lowest-order beam field with a beam waist located at the focal point of a sphere. The focal length f used here is the one which is defined by Gaussian optics. The far-field divergence angles of laser are $13^{\circ} \times 24^{\circ}$ [12]. Since the angular beam spread is related with the spot size of the circular beam, the average spot size can be obtained. The sphere has the refractive index $\sqrt{\varepsilon_r} = 2.0$ and the relative permiability $\mu_r = 1$. The other parameters are $\lambda = 1.55\mu$m, $f = a$, $\chi = 0$, and the smallest spot size of the incident beam is 1.05μm.

Figures 2 and 3 show the scattered near field of the lowest-order incident beam by a chiral sphere (for several different values of the chirality parameter κ) for the cases $a = \lambda$ and $a = 1.3\lambda$, respectively. The chirality parameter $\kappa = 0$ corresponds to a dielectric sphere. The observation plane is another focal plane. From these figures, it is found that the output field of the incident beam are focused and the effective refractive index for a chiral sphere with radius $a = \lambda$ is smaller than that for a dielectric sphere [13] since the output fields for a chiral sphere are more spreaded than that for a dielectric one. Figures 4 and 5 show the scattered near field by a plane wave for a chiral sphere with the same parameters. We also found that for a chiral sphere the diffraction effect for the plane wave is larger than that for the beam incidence.

5. Conclusions

The scattering of a Hermite-Gaussian beam by a chiral sphere has been analyzed by using the relations between the multipole fields and the conventional Hermite-Gaussian beam. The scattered near field of the lowest-order incident beam by a chiral sphere has been calculated numerically and compared with

that of a plane wave incidence. We found that the effective refractive index for a chiral sphere (with radius of 1 wavelength) is smaller than that for a dielectric sphere.

References

[1] I. V. Lindel *et al.*, *Electromagnetic waves in chiral and bi-isotropic media*, Artech House, 1994.
[2] C. F. Bohren, *Chem. Phys. Lett.*, vol. 29, pp. 458–462, 1974.
[3] M. Tanaka and A. Kusunoki, *IEICE Trans. Electron.*, vol. E76–C, pp. 1443–1448, 1993.
[4] K. Matsumoto, K. Rokushima, and J. Yamakita, *IEICE*, vol. J79-C-I, pp. 165–172, 1996.
[5] K. Kunishi, M. Koshiba, and Y. Tsuji, *IEICE*, vol. J82-C-I, pp. 318–325, 1999.
[6] G. A. Deschamps, *Electron. Lett.*, vol. 7, pp. 684–685, 1971.
[7] S. Y. Shin and L. B. Felsen, *J. Opt. Soc. Am.*, vol. 67, pp. 699–700, 1977.
[8] M. Yokota, T. Takenaka, and O. Fukumitsu, *IECE Japan*, vol. J68-C, pp. 1130–1131, 1985.
[9] D. Colton and R. Kress, *Inverse Acoustic and Electromagnetic Scattering Theory*, Springer–Verlag, 1992.
[10] J. S. Kim and S. S. Lee, *J. Opt. Soc. Am.*, vol. 73, pp. 303–312, 1983.
[11] A. E. Siegman, *J. Opt. Soc. Am.*, vol. 63, pp. 1093–1094, 1973.
[12] S. S. Saini *et al.*, *IEEE Photon. Technol. Lett.*, vol. 10, pp. 12132–1234, 1998.
[13] A. H. Sihvola and I. V. Lindel, *J. Electromagn. Waves Appl.*, vol. 6, pp. 553–572, 1992.

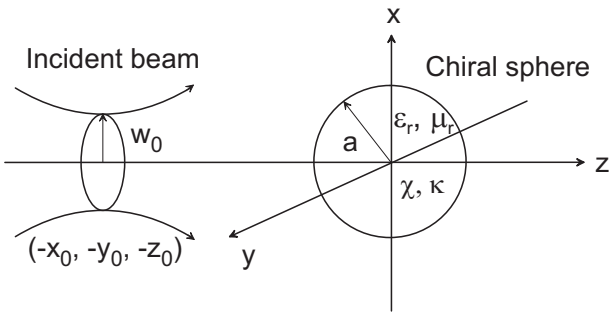

Fig. 1 Geometry of the problem

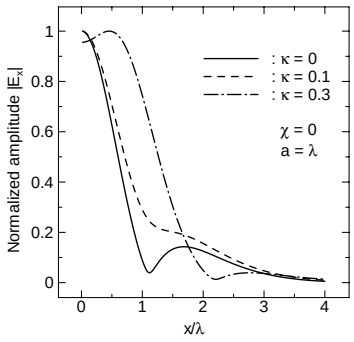

Fig. 2 Scattered near field of the beam field for the radius $a = 1.0\lambda$

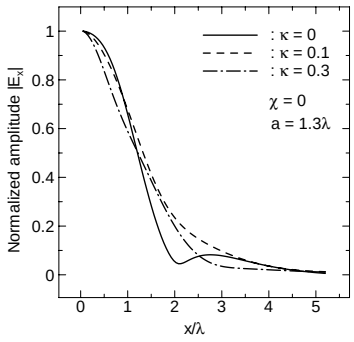

Fig. 3 Scattered near field of the beam field for the radius $a = 1.3\lambda$

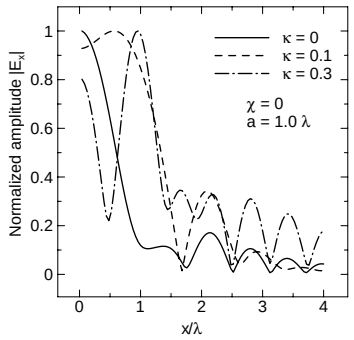

Fig. 4 Scattered near field of the plane wave for the radius $a = 1.0\lambda$

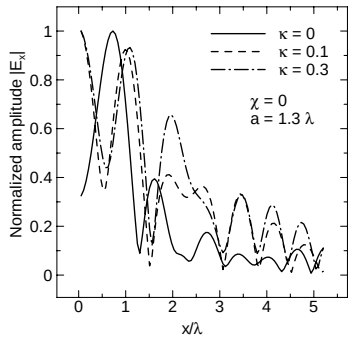

Fig. 5 Scattered near field of the plane wave for the radius $a = 1.3\lambda$